Microfluidics

Polydopamine Microfluidic System toward a Two-Dimensional, Gravity-Driven Mixing Device**

Inseong You, Sung Min Kang, Sunhee Lee, Young Ook Cho, Jin Back Kim, Sang Bok Lee, Yoon Sung Nam,* and Haeshin Lee*

Microfluidics is a multidisciplinary technology that covers many fields ranging from chemistry and biology to electrical engineering. Microfluidic devices allow a variety of typical laboratory operations, such as chemical reactions and biological assays, to be performed rapidly and economically with small volumes of samples.[1–5] These devices enable the synthesis of monodisperse particles, the rapid adjustment of reaction conditions for protein crystallization, and the measurement of enzyme kinetics.[6–10] Conventional microfluidic devices utilize microfabricated 3D poly(dimethylsiloxane) (PDMS) channels on silicon substrates. 2D microfluidic devices called "surface-tension-confined microfluidics" (STCM) devices, which are different from channel-type microfluidic devices, have been introduced.[11–13] The STCM device relies on the alternating patterns of hydrophilic and (super)hydrophobic areas to self-drive or guide the liquid by using the capillary force in the hydrophilic area. In this device, the (super)hydrophobic region acts as a curb that confines the liquid without side walls. The STCM device provides a low-energy method to transport fluids by eliminating the use of a micropump; it also allows easy introduction of fluids onto 2D channels through micropipetting.[14–16] Nevertheless, the long-term stability and various technical limitations of STCM devices should be addressed. A small quantity of moving fluids could remain on the hydrophilic areas of the STCM devices, thus resulting in loss of fluids.[11,17,18] Additionally, the

water-guiding hydrophilic regions are thermodynamically unstable, which is the result of the restoration of hydrophobicity of the hydrophilic, patterned areas by treatment with plasma or UV irradiation.[19,20] Furthermore, creating permanent hydrophilic micropatterns on superhydrophobic surfaces remains challenging.

Herein, we report a new polydopamine-based microfluidic system, which we call polydopamine microfluidic device or pD microfluidic device. It is a pump-free, two-dimensional energy-efficient microfluidic system that is operated with gravity. To the best of our knowledge, the pD microfluidic device is the first example of a truly pump-free and gravity-based automated device that does not require an external energy input. Importantly, the introduction of a droplet-capturing design to the pD microfluidic device enables the very precise control of the mixing of droplets at a relatively fast rate, thus showing 100% mixing efficiency. The 100% droplet mixing allows the pD microfluidic device to perform a 14 mL reaction in only eight minutes, which is an order of magnitude faster than the reaction capacity of conventional microfluidic devices.[21–25]

The device was fabricated by using hydrophilic polydopamine micropatterns on nanostructured, superhydrophobic, anodized aluminum oxide (AAO) surfaces.[26] As a proof-of-concept experiment, we fabricated kinked polydopamine microlines (pD microlines) with a width of 60 μm to test whether the pD microline would confine the droplet movement along the line. The microline was successfully generated by photolithography combined with polydopamine coating before photoresist development (Figure 1a, Figure S1). The area coated by pD does not show the characteristic nanopores of the AAO surfaces (Figure S1b), and exact measurement of the layer thickness is difficult because of the intrinsic roughness of the pD layer. Nonetheless, the scanning electron microscopy (SEM) experiment allowed us to estimate that the thickness is about 200–300 nm (Figure S1c). The pD is utilized for permanent micropatterning on superhydrophobic AAO surfaces, and this application is inspired by the amino acid composition of various adhesive proteins of mussels.[27] It is known that when dopamine molecules are spontaneously polymerized in an alkaline solution, they can modify virtually any type of substrate, including hydrophobic poly(tetrafluoroethylene) (PTFE) and superhydrophobic substrates, by dipping the substrates in the solution.[28–31] The pD coating is stable in aqueous environments as a result of multiple binding mechanisms, including π–π interactions, coordination bonds, and covalent bonds.[32] When the polydopamine-patterned surface was sloped down (at a slope angle θ of 5°), the water droplet moved along the predetermined pD microlines by

[*] I. You, Dr. S. M. Kang, S. Lee, Prof. Dr. H. Lee
Graduate School of Nanoscience & Technology (WCU), KAIST
Daejeon, 305-701 (Republic of Korea)
E-mail: haeshin@kaist.ac.kr
Homepage: http://sticky.kaist.ac.kr

Dr. S. M. Kang, Y. O. Cho, Prof. Dr. H. Lee
Department of Chemistry, KAIST
Daejeon, 305-701 (Republic of Korea)

Prof. Dr. S. B. Lee
Department of Chemistry & Biochemistry, University of Maryland
College Park, Maryland 20742 (USA)

Prof. Dr. Y. S. Nam
Department of Materials Science and Engineering
KAIST Institutes for NanoCentury and BioCentury, KAIST
Daejeon, 305-701 (Republic of Korea)
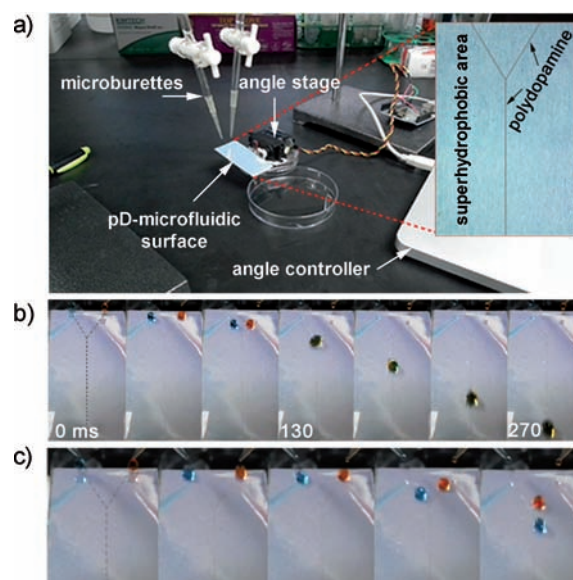E-mail: yoonsung@kaist.ac.kr
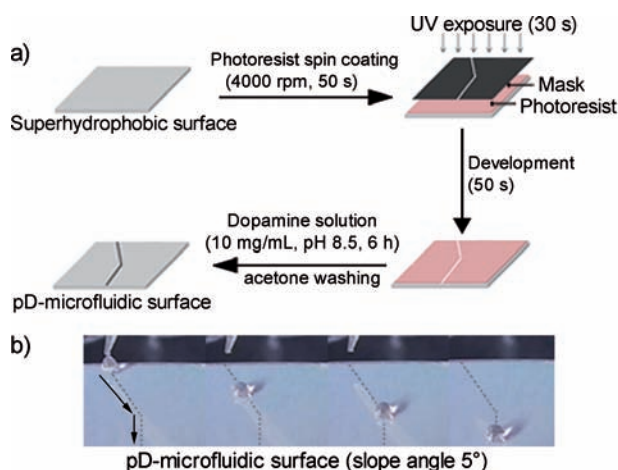
Figure 1. Introduction of permanent hydrophilic pD microlines on superhydrophobic AAO surfaces. a) Introduction of kinked pD microlines on superhydrophobic AAO surfaces (width = 60 μm). b) Monitoring of the movement of a droplet (vol. = 10 μL) on the kinked pD microline.


Figure 2. a) Photograph of the pD microfluidic device. b) Operation of the pD microfluidic device. A droplet of methyl orange (10 μL, pH 4.4, red) and a droplet of bromocresol green (10 μL, pH 5.3, blue) were mixed on the pD microlines (width = 60 μm, slope angle = 5°). c) Failure of droplet mixing because of various unpredictable causes during operation. Even two droplets that were simultaneously applied could not be mixed because of the difference in the speed of the two droplets.

gravity (i.e., without extra energy input; Figure 1 b). The static contact angle of the water droplet on the pD microlines was $(155 \pm 2)°$, which is a feasible contact angle for superhydrophobic surfaces (Figure S2). The high contact angle minimizes the dragging force and eliminates a residual solution on the microlines.[33]

To apply pD microfluidic systems to complex chemical reactions, Y-patterned pD microlines were fabricated on a superhydrophobic AAO surface. This pD microfluidic device consists of microburettes, a pD-patterned surface, a slope angle control stage and a controller, and a collector (Figure 2 a). A droplet of methyl orange (pH 4.4, right) and a droplet of bromocresol green (pH 5.3, left) were simultaneously applied with microburettes; they then travelled along the pD microlines to mix at the intersection point. Next, the neutralization reaction changed the final pH value of the mixture to 4.8, thus turning the mixed solution green (Figure 2 b). The mixing rate was high enough to show the resulting green color immediately after mixing the two droplets (Figure S3). However, in many cases, the droplets failed to mix during the use of the pD microfluidic device. The failure to mix could be a result of several factors: 1) the solutions are not simultaneously dropped from the microburettes; 2) the difference in the physical properties of the fluids (such as viscosity) often creates large surface tension on the tip of the microburettes, thus hindering the simultaneous formation of the droplets; 3) the traveling speed of each individual droplet is different because of the variation in the drag force on the pD microlines (Figure 2 c).

To overcome the mixing problem, we introduced large square micropatches of pD with a width of 200 μm at the intersection of the Y-patterned pD microlines (Figure 3 a). The idea was to provide enough surface energy to capture the first incoming droplet but not enough surface energy to maintain the droplet after the second droplet is mixed. As expected, the first water droplet (10 μL) is captured on the square patch while waiting for the second water droplet

(10 μL) from the other microburette. The droplet starts to move downwards only when the second droplet is mixed with the first droplet (Figure 3 b). This phenomenon can be explained by the force balance relationship between the gravitational force and the surface tension applied to the water droplet (Figure 3 c). The gravitational force (F_g) acting on the droplet is given by $F_g = mg$, in which m is the mass of the droplet, and g is the gravitational acceleration $(9.81 \, \mathrm{m\,s^{-12}})$.

To obtain the surface normal force (F_t), which is a result of the surface tension, an assumption is made: The advancing angle (ϕ_1) and the receding angle (ϕ_2) of the droplet on the inclined surface ($\theta = 5°$) are nearly the same ($\phi = \phi_1 = \phi_2 = 24.9°$, obtained from $180° - 155.1°$, the static contact angle, as shown in Figure S2) because of the very low hysteresis ($\approx 1.4°$).[30] Therefore, the surface normal force is given by $F_t = \gamma D \sin\phi$, in which γ is the surface tension of the water, and D is the perimeter of the circle created by the water/substrate contact. The value of D was obtained by using a fluorescent solution containing fluorescein isothiocyanate (FITC, 0.005 mg mL^{-1}).

The measured D was 1.2 mm for the 10 μL droplet on the pD microline. D was increased to 3.2 mm when the droplet was located on the micropatch. D was further increased to 3.9 mm when the second droplet (20 μL) was mixed on the micropatch. The y component of F_t ($F_{t,y}$) is given by $F_{t,y} = \gamma D \sin\phi \cos\theta$. Before the droplet approached the micropatch, the solution moved downwards because F_g (98.1 μN) was greater than $F_{t,y}$ (43.5 μN). When the droplet was captured by the pD micropatch, $F_{t,y}$ increased from 43.5 μN to 116.0 μN, which was greater than F_g. This increase leads to the water
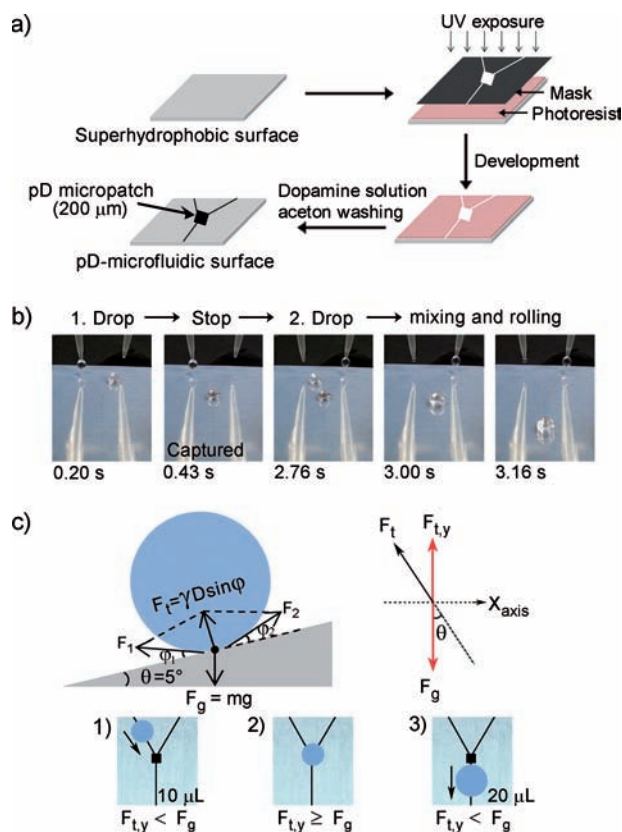
Figure 3. a) Introduction of a square pD micropatch (width = 200 μm) at the intersection of the pD microfluidic surface. b) Overcoming the failure to mix droplets (described in Figure 2 c) by capturing the first droplet (second photo). When the second droplet is mixed (third and fourth photo), the resulting droplet starts to move downwards (fifth photo). c) Mechanical description of the movement and capture of the droplet. When the downward component (F_g) is greater than the upward component ($F_{t,y}$), the droplet moves downwards (shown in parts 1 and 3). When F_g is smaller than $F_{t,y}$, the droplet is captured (shown in part 2).

droplet being captured. Finally, when an additional droplet (10 μL) met the captured droplet, F_g doubled to 196.1 μN, and $F_{t,y}$ increased to 144.6 μN. Because F_g was greater than $F_{t,y}$, the mixed droplet started to move downwards again. The idea for the pD micropatch to hold a droplet can be expanded to create complex multichannel fluidic devices. Introduction of an additional pD micropatch that is bigger in its size compared with the previous patch allows to capture a droplet with larger volume. Thus, new pD microlines that direct to the new patch can be integrated to establish multi-channel devices.

The pD microfluidic device was used to synthesize gold nanoparticles (AuNPs).[34] A droplet of an aqueous solution of gold(III) chloride ($HAuCl_4$, 2 mM, 10 μL) and a droplet of an aqueous solution of sodium borohydride ($NaBH_4$, 10 mM, 10 μL) were introduced to the square micropatch of the pD microfluidic surface. While the initial solutions were transparent, the mixed droplet rapidly developed a red color, the intensity of which increased, thus indicating that AuNPs were formed inside the droplet (Figure 4 a, see also Movie 1 in the Supporting Information). To obtain the kinetic information of

the reaction, the intensity of the red color was calculated. The color of the reaction mixture was analyzed by Adobe Photoshop (CS5). To obtain kinetic information, we used picture frames at intervals of 8 ms. In each individual picture frame, the color of the reaction mixture was divided into red (R), green (G), and blue (B) components. As the red component increased because AuNPs were synthesized, the $R/(G+B)$ value was used as y axis (Figure 4 b). Figure 4 b clearly shows synthesis of AuNPs in the mixed droplet, as the intensity of red color denoted by $R/(G+B)$ increased. After 200 ms, the developing red color was saturated, thus indicat-
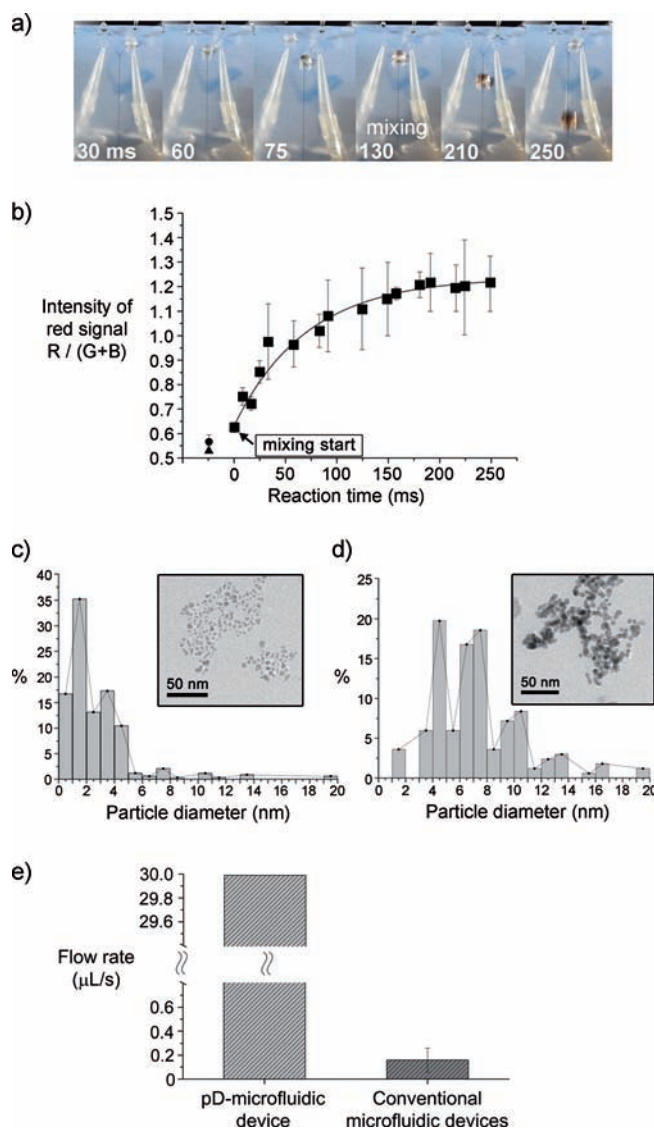
Figure 4. Synthesis of AuNPs using the pD microfluidic device. a) A droplet of $HAuCl_4$ (10 μL, 2 mM, right) and a droplet of $NaBH_4$ (10 μL, 10 mM, left) were mixed (fourth photo). The color of the mixed droplet rapidly changed into red (fifth and sixth photo). b) Kinetic analysis on the synthesis of AuNPs (square: mixed droplet, circle: droplet of $NaBH_4$ before mixing, and triangle: droplet of $HAuCl_4$ before mixing). Histograms ($n=450$) of AuNPs synthesized by c) the pD microfluidic device (TEM image, inset) and d) bulk mixing (TEM image, inset). e) Comparison between the flow rate used in pD microfluidic system versus the ones in conventional microfluidic devices.

ing that AuNP synthesis was completed. For a control experiment, we performed a typical bulk reaction (vol = 14 mL). The synthesized AuNPs were analyzed by transmission electron microscopy (TEM). The AuNPs synthesized by the pD microfluidic device show a narrower size distribution compared with those prepared by the bulk reaction (Figure 4c and d). Also, the size of AuNPs collected from pD microfluidic device is smaller than that of AuNPs prepared by the bulk reaction (Figure 4c and d, insets). The enhanced monodispersity of AuNPs synthesized by the pD microfluidic device might be a result of the decreased diffusion path length within the droplet, which results in rapid and homogeneous mixing.[35] This result shows that the pD microfluidic device can be utilized as a new, promising micro-reactor for the synthesis of nanoparticles with a monodisperse size distribution. Importantly, the flow rate of pD microfluidic devices (30 µLs^{-1}) is higher than that of conventional droplet-based, three-dimensional microfluidic systems (≈ 0.2 µLs^{-1}),[21–25] thus making pD microfluidic devices suitable for large-scale applications (Figure 4e).

Fast induction of the structural change of a protein was demonstrated as another potential application of the pD microfluidic device. We used a photoactive yellow protein (PYP) as a model system because of its bright yellow color ($\lambda_{max} = 446$ nm, $\varepsilon_{446} = 45.5$ mM^{-1}cm^{-1}).[36] PYP loses the yellow color when it is denatured because of the protonation at the hydroxy group of *p*-coumaric acid.[37,38] A droplet of PYP solution (10 µL, 0.2 mM) and a droplet of guanidine hydrochloride solution (GuHCl, 10 µL, 1M) were mixed on the pD microfluidic surface. The bright yellow color disappeared when the denaturant GuHCl was mixed with the PYP solution. The denaturation kinetics of PYP was obtained by using the R/G/B color component division method described in Figure 4b using Adobe Photoshop. Instead of R/(G+B), we used (R + G)/B, as yellow is a mixture of red and green (Figure S4). The denaturation reaction of PYP was completed after about 80 ms. The real-time monitoring of the rapidly changing structure of PYP by the colorimetric analysis demonstrates the power of the pD microfluidic device as a new approach to the study of protein folding and unfolding.

In conclusion, we demonstrated a new surface-tension-confined droplet microfluidic device, called "pD microfluidic system". Spatially controlled modification of the AAO super-hydrophobic surface through mussel-inspired pD coating generates hydrophilic microlines on the surface. On the pD microlines, movement and mixing of droplets are precisely controlled in an energy-efficient manner by gravity. The narrow pD microlines on the superhydrophobic AAO surfaces result in the minimization of dragging force as well as in no residual traces of solutions. Considering previously reported wettability switchable surfaces by electric potential or smart polymers, further intelligent designs of polydopamine microfluidic devices are worth pursuing.[39,40] Introduction of a pD square patch at the intersection of the Y-patterned pD microlines enables one to control the movement of a droplet, such as stopping and starting movement. This micropatch allows 100% droplet mixing. The pD microfluidic device is used to synthesize monodisperse nanoparticles and rapidly induce structural changes of a protein. This

microfluidic system has a great potential as a new category of pump-free microfluidic systems that can be used in various applications.

[1] G. M. Whitesides, *Nature* **2006**, *442*, 368–373.

[2] T. Thorsen, S. J. Maerkl, S. R. Quake, *Science* **2002**, *298*, 580–584.

[3] K. Jähnisch, V. Hessel, H. Lowe, M. Baerns, *Angew. Chem.* **2004**, *116*, 410–451; *Angew. Chem. Int. Ed.* **2004**, *43*, 406–447.

[4] M. A. Powers, S. T. Koev, A. Schleunitz, H. Yi, V. Hodzic, W. E. Bentley, G. F. Payne, G. W. Rubloff, R. Ghodssi, *Lab Chip* **2005**, *5*, 583–586.

[5] J. J. Park, X. Luo, H. Yi, T. M. Valentine, G. F. Payne, W. E. Bentley, R. Ghodssi, G. W. Rubloff, *Lab Chip* **2006**, *6*, 1315–1321.

[6] H. C. Shum, J. W. Kim, D. A. Weitz, *J. Am. Chem. Soc.* **2008**, *130*, 9543–9549.

[7] A. R. Abate, M. Kutsovsky, S. Seiffert, M. Windbergs, L. F. V. Pinto, A. Rotem, A. S. Utada, D. A. Weitz, *Adv. Mater.* **2011**, *23*, 1757–1760.

[8] W. D. Ristenpart, J. Wan, H. A. Stone, *Anal. Chem.* **2008**, *80*, 3270–3276.

[9] P. Dextras, K. R. Payer, T. P. Burg, W. Shen, Y. C. Wang, J. Y. Han, S. R. Manalis, *J. Microelectromech. Syst.* **2011**, *20*, 221–230.

[10] M. Srisa-Art, A. J. deMello, J. B. Edel, *Anal. Chem.* **2007**, *79*, 6682–6689.

[11] P. Lam, K. J. Wynne, G. E. Wnek, *Langmuir* **2002**, *18*, 948–951.

[12] H. Gau, S. Herminghaus, P. Lenz, R. Lipowsky, *Science* **1999**, *283*, 46–49.

[13] B. Zhao, J. S. Moore, D. J. Beebe, *Science* **2001**, *291*, 1023–1026.

[14] M. J. Swickrath, S. Shenoy, J. A. Mann, Jr., J. Belcher, R. Kovar, G. E. Wnek, *Microfluid. Nanofluid.* **2008**, *4*, 601–611.

[15] S. Chao, D. R. Meldrum, *Lab Chip* **2009**, *9*, 867–869.

[16] M. Grunze, *Science* **1999**, *283*, 41–42.

[17] S. Bouaidat, O. Hansen, H. Bruus, C. Berendsen, N. K. Bau-Madsen, P. Thomsen, A. Wolff, J. Jonsmann, *Lab Chip* **2005**, *5*, 827–836.

[18] N. J. Shirtcliffe, G. McHale, M. I. Newton, *Langmuir* **2009**, *25*, 14121–14128.

[19] X. Feng, L. Feng, M. Jin, J. Zhai, L. Jiang, D. Zhu, *J. Am. Chem. Soc.* **2004**, *126*, 62–63.

[20] N. M. Oliveira, A. I. Neto, W. Song, J. F. Mano, *Appl. Phys. Express* **2010**, *3*, 085205.

[21] L. Frenz, J. Blouwolff, A. D. Griffiths, J. C. Baret, *Langmuir* **2008**, *24*, 12073–12076.

[22] H. Song, R. F. Ismagilov, *J. Am. Chem. Soc.* **2003**, *125*, 14613–14619.

[23] D. L. Chen, C. J. Gerdts, R. F. Ismagilov, *J. Am. Chem. Soc.* **2005**, *127*, 9672–9673.

[24] H. Song, M. R. Bringer, J. D. Tice, C. J. Gerdts, R. F. Ismagilov, *Appl. Phys. Lett.* **2003**, *83*, 4664–4666.

[25] H. Song, J. D. Tice, R. F. Ismagilov, *Angew. Chem.* **2003**, *115*, 792–796; *Angew. Chem. Int. Ed.* **2003**, *42*, 768–772.

[26] W. K. Cho, S. Park, S. Jon, I. S. Choi, *Nanotechnology* **2007**, *18*, 395602.

[27] J. H. Waite, *Nat. Mater.* **2008**, *7*, 8–9.

[28] H. Lee, S. M. Dellatore, W. M. Miller, P. B. Messersmith, *Science* **2007**, *318*, 426–430.

[29] F. Bernsmann, A. Ponche, C. Ringwald, J. Hemmerle, J. Raya, B. Bechinger, J. C. Voegel, P. Schaaf, V. Ball, *J. Phys. Chem. C* **2009**, *113*, 8234–8242.

[30] S. M. Kang, I. You, W. K. Cho, H. K. Shon, T. G. Lee, I. S. Choi, J. M. Karp, H. Lee, *Angew. Chem.* **2010**, *122*, 9591–9594; *Angew. Chem. Int. Ed.* **2010**, *49*, 9401–9404.

[31] S. Hong, K. Y. Kim, H. J. Wook, S. Y. Park, K. D. Lee, D. Y. Lee, H. Lee, *Nanomedicine* **2011**, *6*, 793–801.

[32] H. Lee, N. F. Scherer, P. B. Messersmith, *Proc. Natl. Acad. Sci. USA* **2006**, *103*, 12999–13003.

[33] C. H. Choi, C. J. Kim, *Phys. Rev. Lett.* **2006**, *96*, 066001.

[34] S. Duraiswamy, S. A. Khan, *Small* **2009**, *5*, 2828–2834.

[35] S. Y. Teh, R. Lin, L. H. Hung, A. P. Lee, *Lab Chip* **2008**, *8*, 198–220.

[36] T. Meyer, *Biochim. Biophys. Acta Bioenerg.* **1985**, *806*, 175–183.

[37] H. F. Arata, F. Gillot, T. Nojima, T. Fujii, H. Fujita, *Lab Chip* **2008**, *8*, 1436–144.

[38] W. D. Hoff, B. Devreese, R. Fokkens, I. M. Nugteren-Roodzant, J. V. Beeumen, N. Nibbering, K. J. Hellingwerf, *Biochemistry* **1996**, *35*, 1274–1281.

[39] J. Lahann, S. Mitragotri, T. N. Tran, H. Kaido, J. Sundaram, I. S. Choi, S. Hoffer, G. A. Somorjai, R. Langer, *Science* **2003**, *299*, 371–374.

[40] M. C. LeMieux, Y. H. Lin, P. D. Cuong, H. S. Ahn, E. R. Zubarev, V. V. Tsukruk, *Adv. Funct. Mater.* **2005**, *15*, 1529–1540.